J Anesth (2012) 26:54–61
DOI 10.1007/s00540-011-1260-y

ORIGINAL ARTICLE

Clinical dose of lidocaine destroys the cell membrane and induces both necrosis and apoptosis in an identified *Lymnaea* neuron

Shin Onizuka · Ryuji Tamura · Tetsu Yonaha · Nobuko Oda · Yuko Kawasaki · Tetsuro Shirasaka · Seiji Shiraishi · Isao Tsuneyoshi

Received: 3 February 2011 / Accepted: 6 October 2011 / Published online: 29 October 2011

Abstract
Purpose Although lidocaine-induced cell toxicity has been reported, its mechanism is unclear. Cell size, morphological change, and membrane resistance are related to homeostasis and damage to the cell membrane; however, the effects of lidocaine on these factors are unclear. Using an identified LPeD1 neuron from *Lymnaea stagnalis*, we sought to determine how lidocaine affects these factors and how lidocaine is related to damage of the cell membrane.
Methods Cell size and morphological form were measured by a micrograph and imaging analysis system. Membrane potential and survival rate were obtained by intracellular recording. Membrane resistance and capacitance were measured by whole-cell patch clamp. Phosphatidyl serine and nucleic acid were double stained and simultaneously measured by annexin V and propidium iodide.
Results Lidocaine at a clinical dose (5–20 mM) induced morphological change (bulla and bleb) in the neuron and increased cell size in a concentration-dependent manner. Membrane potential was depolarized in a concentration-dependent manner. At perfusion of more than 5 mM lidocaine, the depolarized membrane potential was irreversible. Lidocaine decreased membrane resistance and increased membrane capacitance in a concentration-dependent manner. Both phosphatidyl serine and nucleic acid were stained under lidocaine exposure in a concentration-dependent manner.
Conclusions A clinical dose of lidocaine greater than 5 mM destroys the cell membrane and induces both necrosis and apoptosis in an identified *Lymnaea* neuron.

Keywords Lidocaine · Necrosis · Apoptosis · Annexin

Introduction

Lidocaine is commonly used for regional anesthesia and postoperative pain relief. However, neural injury after spinal anesthesia initially seems to result from the specific effects of lidocaine, because most reported cases of cauda equina syndrome have occurred in patients who have received spinal anesthesia using this agent [1–3]. Anesthesiologists have become concerned about irreversible neural injury caused by lidocaine. To clarify the mechanisms of such neurotoxicity, numerous studies have been performed in the fields of animal behavior, electrophysiology, and histopathology [4, 5]. We have also reported that lidocaine induced neurotoxicity with morphological changes such as cell axon collapse and cell swelling [6, 7]. It has been demonstrated that one of the mechanisms of neurotoxicity by lidocaine is apoptosis through the mitochondrial pathway [8, 9]. We have also reported that lidocaine induces apoptosis through the mitochondrial pathway by intracellular alkalization and increases in intracellular calcium and sodium [10–12]. In contrast, lidocaine-induced necrosis has also been reported [13, 14]. Increases in intracellular Ca^{2+}, Na^{+}, and pH can result in apoptosis or necrosis [15–17]. For example, dynamic

S. Onizuka (✉) · R. Tamura · T. Yonaha · N. Oda · Y. Kawasaki · T. Shirasaka · I. Tsuneyoshi
Department of Anesthesiology and Intensive Care, Faculty of Medicine, University of Miyazaki, Kiyotake-Cho, Miyazaki 889-1692, Japan
e-mail: pirotann@med.miyazaki-u.ac.jp

S. Shiraishi
Innovative Pathophysiology Research Group, Division of Cancer Pathophysiology, National Cancer Center Research Institute, 5-1-1 Tsukiji, Chuo-ku, Tokyo 104-0045, Japan

membrane blebbing is caused by the increased contractility of the acto-myosin system following myosin light chain (MLC) phosphorylation. MLC phosphorylation is a consequence of the cleavage of a Rho GTPase effector, the kinase ROCK I, by caspase-3 activation, and this caspase-3 activation is brought about by these intracellular Ca^{2+}, Na^{+}, and pH increases [18–20]. However, different kinds of evidence and many mechanisms for lidocaine-induced apoptosis and necrosis have been presented. Commonly, in necrosis, cell size is increased and cell swelling occurs, whereas cell size is decreased in apoptosis [21, 22]. We speculate that irreversible nerve injury results from the direct destruction of the cell membrane by lidocaine. To demonstrate this hypothesis, morphological changes such as cell size, survival rate, membrane potential, membrane resistance, cell capacitance, and induction of apoptosis or necrosis by lidocaine were examined.

Materials and methods

Animal and cell culture

All animal experiments were approved by the Animal Care Committee of the University of Miyazaki. Specifically, individually identified left pedal dorsal 1 (LPeD1) neurons from laboratory-raised *Lymnaea stagnalis* (freshwater snail) were used at room temperature. The snails were deshelled and transferred to a sterile dissection dish in normal *Lymnaea* saline [51.3 mM NaCl, 1.7 mM KCl, 4.1 mM $CaCl_2$, 1.5 mM $MgCl_2$, and 5.0 mM *N*-2-hydroxyethylpiperazine-*N*-2-ethanesulfonic acid (HEPES), pH 8, with NaOH]. The ganglia were treated in a defined medium [serum-free 50% Leibovitz L-15 medium (GIBCO-BRL Life Technologies, Burlington, Ontario, Canada) with added inorganic salts, 20 μg/ml gentamycin, pH 7.9] for 25 min with 0.2% trypsin (type III; Sigma Chemical, St. Louis, MO, USA). The neurons were removed by gentle suction with a siliconized, microforge fine-polished pipette with outside diameter of 1.5 mm (IB-150 F; WPI, Sarasota, FL, USA). The neurons then were transferred to poly-L-lysine-coated culture dishes (Falcon Plastics, Los Angeles, CA, USA) with 3 ml of the defined medium [23].

Measurement of cell size

For comparison, the cell sizes were measured before and after 10 min lidocaine perfusion. Cells were photographed using a Sony XC-003 3CCD digital camera attached to a microscope (Nikon TE-300). Sample cells from the digital images were analyzed on a PC computer using the public domain image analysis program developed at the U.S. National Institutes of Health (NIH Image; Scion, Frederick, MD, USA). The recorded images were saved in a Scion-compatible TIFF format and then imported into the program. Calibration was performed for each image by drawing a line over the scale that was introduced into the image field before digitization [24]. With the line tool, the areas of the sample cells were automatically drawn and measured. The output of the measured areas was transferred to an Excel program to calculate mean areas.

Intracellular recording

Neuronal activity was monitored using conventional intracellular recording [25]. A glass microelectrode with a filament and an outside diameter of 1.5 mm (TW150F-4; WPI) was filled with a KCl pipette solution consisting of 50 mM KCl, 10 mM HEPES, and 2 mM ATP-Mg. The pH was clamped to 7.0 with KOH, yielding a tip resistance of 20–30 MΩ. Electrical signals were amplified with a current–voltage clamp amplifier (Multiclamp-700A; Axon Instruments, Union City, CA, USA). For control and data acquisition, an AD and DA converter (Digidata 1322A; Axon Instruments) was used. Data acquisition and analysis were conducted using pClamp 9 software (Axon Instruments). Lidocaine was perfused for 10 min at each concentration. Live LPeD1 cells have membrane potential less than −50 mV and induce depolarization by current stimulation; however, in contrast, apoptotic or necrotic cells lose their membrane potential and do not depolarize by current stimulation. Therefore, after 60-min washout, the survival rate, defined as "survive," was calculated through observation by recovery of the membrane potential to less than −50 mV and depolarization by 0.5-nA current injection.

Membrane resistance measurement by patch-clamp recordings

Whole-cell patch-clamp recordings in the *Lymnaea* neuron were made using a multiclamp 700 A amplifier (Axon Instruments) [26, 27]. Patch electrodes (tip diameter adjusted to 1.0 μm; resistance, 1–3 MΩ) were pulled from glass tubing (outside diameter, 1.5 mm) with no filament (PG-150T-7.5; Warner Instrument, Hamden, CT, USA) on a vertical pipette puller (PA-10; Narishige, Tokyo, Japan). For control and data acquisition, an AD and DA converter interface board (Digidata 1322A; Axon Instruments) was inserted into a personal computer. Data acquisition and analysis were conducted using pClamp 9 software (Axon Instruments). The current was filtered at 1 kHz using a 4-pole Bessel filter and digitized at a sampling frequency of 20 kHz. To study membrane resistance and capacitance, pipettes were filled with a standard potassium pipette solution consisting of 50 mM KCl, 5 mM ethylene glycol tetraacetic acid (EGTA), 10 mM HEPES, and 2 mM

ATP-Mg; pH was adjusted to 7.4 (with KOH). For whole-cell patch clamp, after obtaining a gigaohm seal, the membrane was ruptured by suction with a syringe, and then the membrane resistance and membrane capacitance were continuously recorded. All experiments were performed at room temperature (20–22°C).

Double staining with propidium iodide and annexin V

An analysis of phosphatidyl serine on the outer leaflet of apoptotic cell membranes was performed using annexin V-FITC to identify apoptotic cells. Necrotic cells were identified by propidium iodide [28]. Each sample cell was incubated with 1 ml staining solution with 10 μM annexin V-FITC and 10 μM propidium iodide in normal saline for 15 min. Evaluation was by fluorescence microscopy using 488 nm excitation and emission at 505 nm for annexin V-FITC and at 590 nm for propidium iodide.

Experimental procedure

In each trial, lidocaine (1, 5, 10, 15, or 20 mM) was perfused into the culture dish for 10 min after the baseline values were measured.

Statistical analysis

The results are expressed as the mean ± standard deviation (SD). Plots were fitted to a Hill equation of the form $y = \text{base} + (\text{max–base})/[1 + (\text{Xhalf/X})^{\text{rate}}]$, where the rate is the Hill coefficient and Xhalf is the half-maximal response (EC_{50}), calculated using Igor Pro software (Version 5.01; WaveMetrics, Tigard, OR, USA).

The results of repeated measurements at each dose for each group of trials were analyzed by repeated-measures one-way analysis of variance (ANOVA), followed by Scheffe's test. StatView (version 4.5; Abacus, Canoga Park, CA, USA) was used for these analyses. $P < 0.05$ was considered to be statistically significant.

Results

Morphological changes by lidocaine

Figure 1a presents photographs of an LPeD1 neuron before and after administration of each concentration of lidocaine. Lidocaine concentration-dependently increased the cell size with E_{max} of 137% ± 11% at 20 mM and EC_{50} 8.6 mM.

Swelling and blebbing were induced in each neuron in a concentration-dependent manner (Fig. 1a,b).

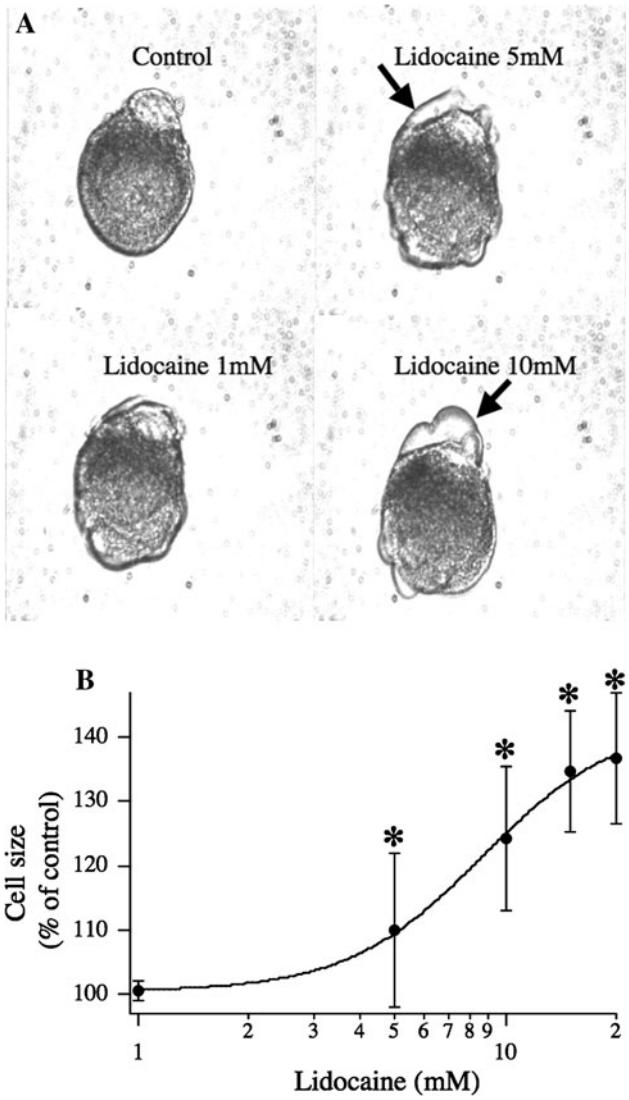

Fig. 1 **a** Morphological changes before and after lidocaine perfusion for 10 min at each concentration. **b** Areas of the sample cells were measured and analyzed by using NIH imaging. Results are presented as mean ± SD, $n = 5$. *$P < 0.05$ in comparison to control values

Irreversible depolarization by lidocaine

Lidocaine induced membrane depolarization in a concentration-dependent manner to −62 ± 11 mV at control, −52 ± 8 at 1 mM, −35 ± 8 at 5 mM, −8 ± 8 at 10 mM, −8 ± 8 at 10 mM, 1.4 ± 3 at 15 mM, and 2.5 ± 3 at 20 mM, with a half-maximal response at 6.2 mM (Fig. 2b). Depolarization at more than 5 mM lidocaine was irreversible after washout for 60 min. In contrast, with 1 mM lidocaine perfusion for 10 min, membrane depolarization recovered after washout (Fig. 2a). Figure 2c shows survival rates 60 min after washout. The effective dose for 50% fatality (ED_{50}) was 7.5 mM.

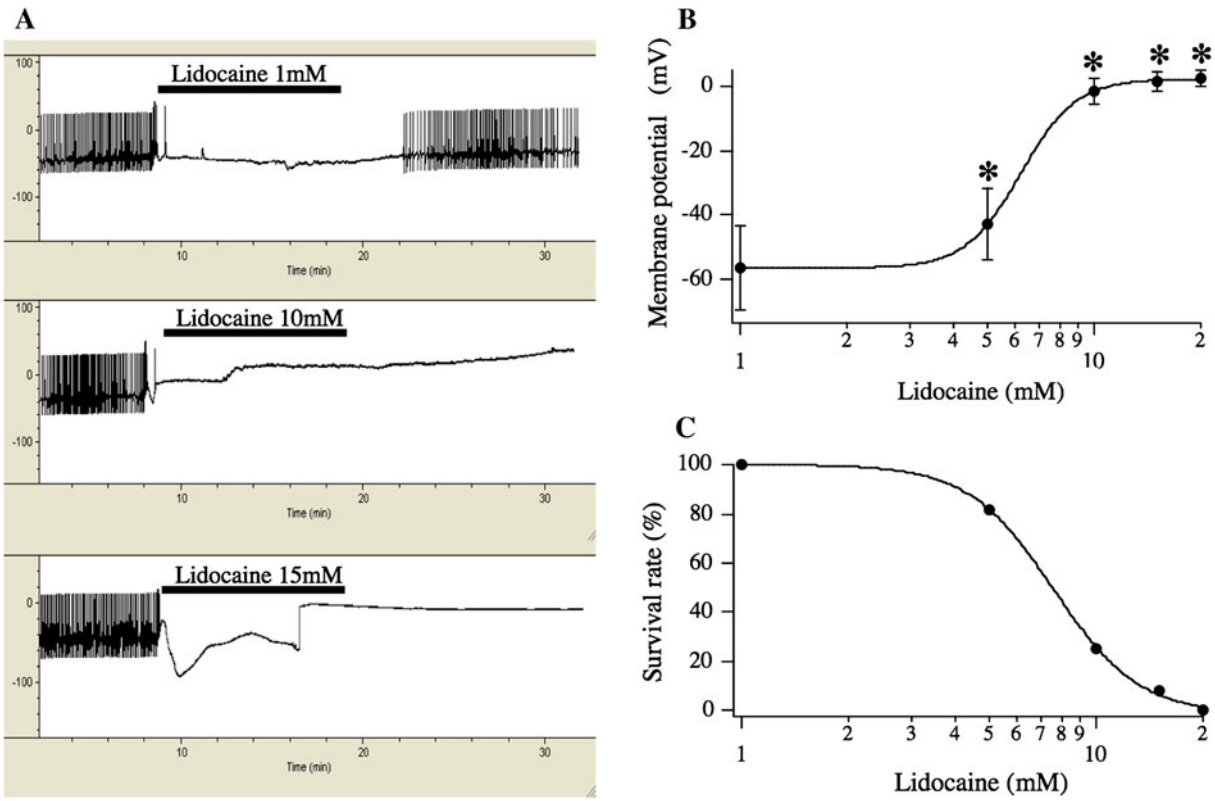

Fig. 2 **a** Lidocaine exposure greater than 10 mM for 10 min induced irreversible depolarization. **b** Graph shows the resting membrane potential of an LPeD1 cell. Lidocaine greater than 10 mM irreversibly depolarized membrane potential toward 0 mV. Results are presented as mean ± SD, $n = 6$ in each concentration. $^*P < 0.05$ in comparison to baseline values. **c** Survival rate of an LPeD1 cell after lidocaine exposure for 10 min at each concentration

Membrane resistance and capacitance measurement

Whole-cell membrane resistance and capacitance were measured by the whole-cell patch-clamp method. Figure 3a shows the experimental tracings of membrane resistance (upper trace) and capacitance (lower trace) before and after 10 mM lidocaine administration. Following lidocaine perfusion, membrane resistance was significantly decreased by 10 and 20 mM lidocaine: whole-membrane resistance changed from 1.4 ± 0.2 (GΩ) at the baseline to 1.2 ± 0.2 at 1 mM, 1.1 ± 0.2 at 5 mM, 0.5 ± 0.2 at 10 mM, 0.3 ± 0.1 at 15 mM, and 0.3 ± 0.2 at 20 mM, with a half-maximal response at 8.0 mM (Fig. 3b). In contrast, whole-membrane capacitance was significantly increased by 10 and 20 mM lidocaine, from 226 ± 52 (pF) at the baseline to 234 ± 54 at 1 mM, 244 ± 57 at 5 mM, 279 ± 66 at 10 mM, 294 ± 30 at 15 mM, and 301 ± 34 at 20 mM, with a half-maximal response at 7.7 mM (Fig. 3c).

Double staining with propidium iodide and annexin V-FITC

Figure 4a shows double staining with propidium iodide and Annexin V-FITC and imaging of an LPeD1 neuron before and after 10 mM lidocaine administration. The fluorescence of propidium iodide was increased faster than that of annexin V-FITC (Fig. 4a). In both propi dium iodide and annexin V-FITC, the fluorescent intensity level was significantly increased after lidocaine exposure for 10 min in a concentration-dependent manner (Fig. 4b). For propidium iodide (PI) staining, ED_{50} was 7.1 mM; for annexin V staining, ED_{50} was 7.2 mM.

Discussion

In the present study, lidocaine induced morphological swelling and irreversible depolarization in a neuron (Figs. 1, 2). To demonstrate whether lidocaine induced membrane destruction, membrane resistance and capacitance were measured. As measured by the whole-cell patch-clamp method, lidocaine decreased membrane resistance and increased capacitance (Fig. 3). Lidocaine induced staining for nucleic acid by propidium iodide, which is one of the markers of necrosis (Fig. 4). Lidocaine also induced phosphatidyl serine exhibition at the cell surface, a marker of early-stage apoptosis (Fig. 4). These

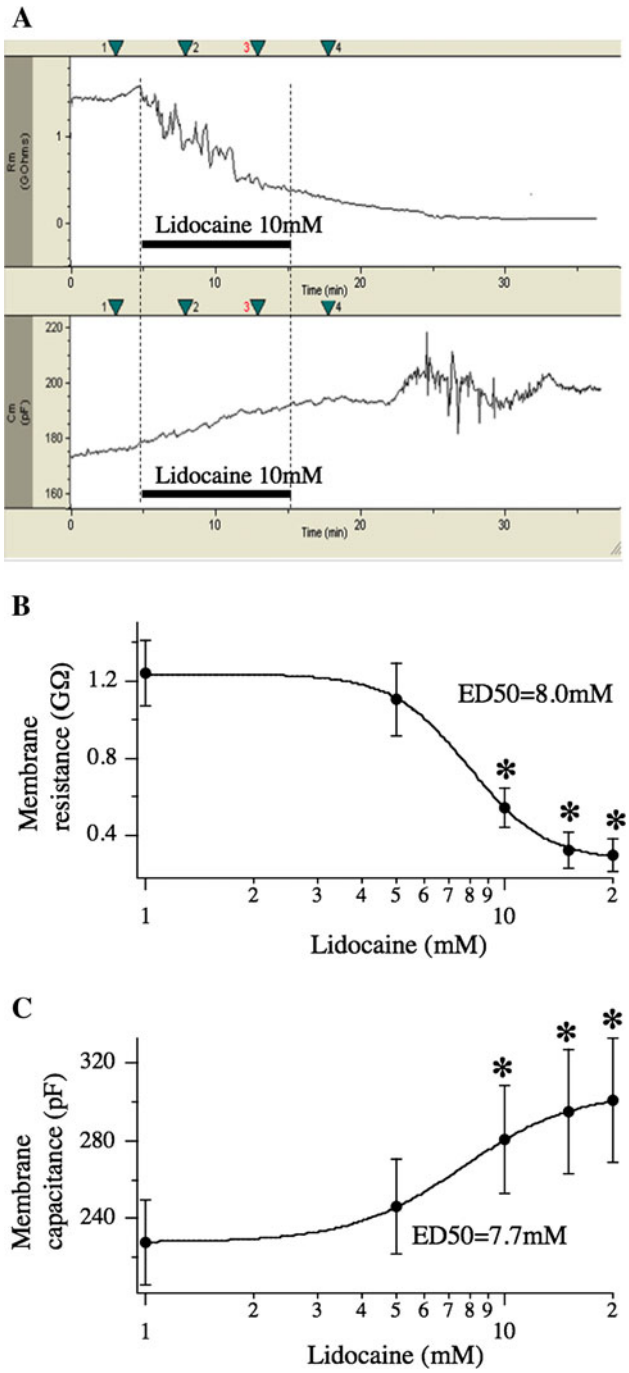

Fig. 3 **a** *Upper trace* shows that lidocaine exposure above 10 mM for 10 min decreased membrane resistance irreversibly. *Lower trace* shows that lidocaine exposure increased membrane capacitance irreversibly. **b** Graph of membrane resistance. Results are presented as mean ± SD, $n = 6$ in each concentration. $^*P < 0.05$ in comparison to baseline values. **c** Graph of membrane capacitance of an LPeD1 cell. Results are presented as mean ± SD, $n = 6$ in each concentration. $^*P < 0.05$ in comparison to baseline values

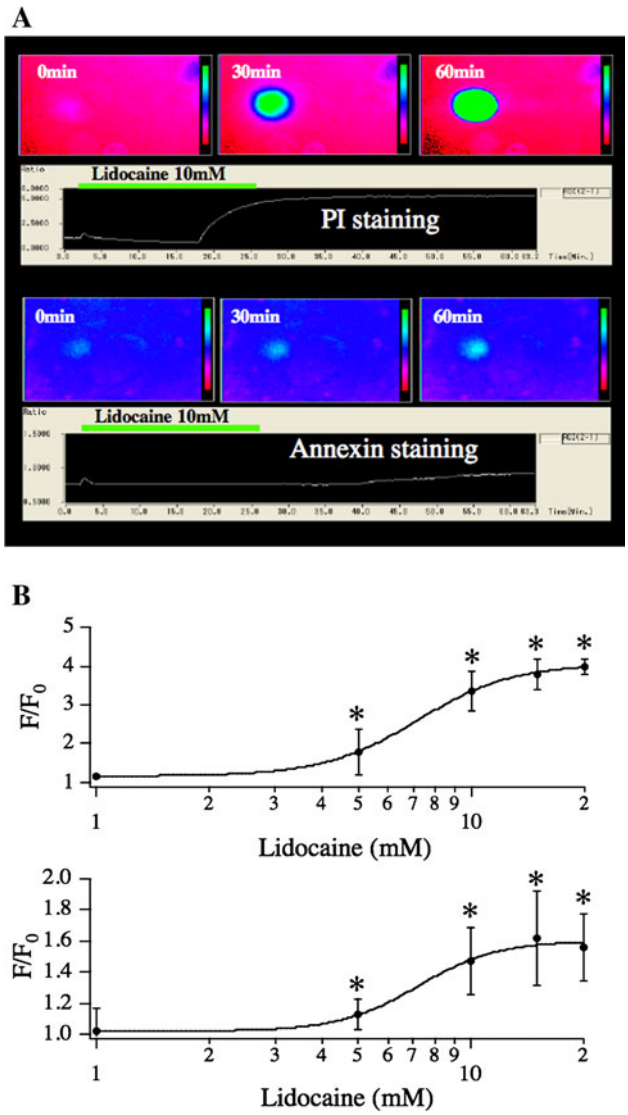

Fig. 4 **a** Fluorescence intensities of propidium iodide (*PI*) and *annexin* V-FITC were measured simultaneously. *Upper trace* and *graph* show fluorescence intensity of propidium iodide (PI); *lower trace* and *graph* show fluorescence intensity of annexin V-FITC before and after lidocaine exposure in the same LPeD1 cell. **b** *Upper graph* fluorescence intensity of PI; *lower graph* fluorescence intensity of annexin V-FITC. Results are presented as mean ± SD, $n = 6$ in each concentration. $^*P < 0.05$ in comparison to baseline values

results indicate that clinical doses of lidocaine at more than 5 mM destroy the cell membrane and induce both apoptosis and necrosis in a neuronal cell.

Many studies have indicated that local anesthetics, especially lidocaine, induce apoptosis or necrosis in neuronal cells, and many mechanisms for the cell toxicity of lidocaine have been investigated. Using frog sciatic nerve, Bainton and Strichartz demonstrated a reduction in compound action potential at 40 mM (1%) lidocaine, with complete ablation at 80 mM lidocaine after washout [29]. Similarly, Kanai et al. reported that a high concentration of lidocaine (80 mM) induced irreversible depolarization, and they concluded that lidocaine had a direct neurotoxic effect

on crayfish giant axons in vitro [30]. These findings suggest that a high concentration of lidocaine may induce transient or permanent neurological deficits, particularly in nerves already jeopardized by direct needle trauma during spinal anesthesia. Werdehausen et al. [8] compared the toxicity of local anesthetics by double-staining assay with 7-amino-actinomycin D (7-AAD) and annexin V measured by flow cytometry in the human neuroblastoma SK-N-SH cell line. They reported that local anesthetics induced about 20% apoptosis and that toxicity was correlated with octanol/buffer coefficients, indicating lipophilicity. Kamiya et al. [31] reported that below 12 mM, lidocaine exposure for 24 h induced about 50% apoptosis in U937 human leukemia cells. Friederich and Schmitz [32] reported that 24-h exposure to 3 mM lidocaine induced about 40% apoptosis in human neuronal SH-SY5Y cells. Lidocaine and mepivacaine exposure increased the number of apoptotic cells significantly more than other anesthetics. At a high concentration (greater than 5 mM), the number of necrotic cells increased. Although many theories have been reported, whether apoptosis or necrosis is primarily induced by lidocaine has been unclear. One reason is that in most of the studies of apoptosis by lidocaine, samples were obtained at 6–24 h after lidocaine exposure, making it difficult to determine whether apoptosis or necrosis was the primary occurrence. The current experiment is the first to provide evidence that lidocaine induces both apoptosis and necrosis in the same neuron within 60 min of lidocaine exposure.

It is generally accepted that cell death can result from either a passive degenerative process (necrosis) or an active process (apoptosis). A multitude of methods, each of them suitable to different experimental conditions, have been described to identify apoptotic cells by flow cytometric analysis [33]. Flow cytometry is the technique of choice for the quantification of apoptosis. One general problem that always arises with the flow cytometric analysis of apoptosis, however, is the distinction between necrotic and apoptotic cells. Moreover, although necrotic cells are usually thought to contaminate objects during the quantification of apoptosis, it is interesting to quantify both apoptosis and necrosis in a given cell population. Although there is no clear-cut parameter that allows the separation by flow cytometry of necrotic from apoptotic cells, particularly at their late stages, such a distinction is immediate with morphological techniques. The presence of apoptotic cells in a given population should always be validated by morphological observations. Therefore, morphological observations from different perspectives under a microscope are important for the identification of apoptosis and its distinction from necrosis.

In apoptotic cells, the membrane phospholipid phosphatidylserine (PS) is translocated from the inner to the outer leaflet of the plasma membrane, thereby exposing PS to the external cellular environment. Annexin V is a 35–36 kDa Ca^{2+}-dependent phospholipid-binding protein that has a high affinity for PS and binds to cells with exposed PS. Annexin V may be conjugated to fluorochromes, including fluorescein isothiocyanate (FITC). This format retains its high affinity for PS and thus serves as a sensitive probe for flow cytometric analysis of cells undergoing apoptosis. Because the externalization of PS occurs in the early stages of apoptosis, FITC annexin V staining can identify apoptosis at an earlier stage than assays based on nuclear changes such as DNA fragmentation. On the other hand, necrosis occurs when the cell membrane loses its integrity and becomes leaky. Therefore, necrotic cells are easily stained with propidium iodide.

Tsuchiya et al. [34] demonstrated that lidocaine induced inflammation through changes in membrane fluidity, supporting the theory of Kitagawa et al. [35] that cytotoxic local anesthetics are amphiphilic molecules that will melt lipid bilayers as detergents and induce necrosis. On the other hand, we previously reported that local anesthetics, especially lidocaine, increase intracellular pH, thus affecting homeostasis [10]. Mitochondria are especially affected and depolarized by intracellular pH changes and will trigger apoptosis or necrosis [36–38].

In the present study, the concentration of lidocaine was established for clinical use; however, lidocaine induced irreversible toxic effects. In clinical practice, 40–80 mM (1–2%) of lidocaine is used; therefore, a high concentration of lidocaine may accumulate in a local area and induce neurological damage. This discrepancy between experimentally effective concentrations for anesthetic actions and those for toxic doses must be considered: 10 mM lidocaine is considered to be a clinically acceptable concentration. Ross et al. and Rigler and Drasner [39, 40] reported that spinal injection with 5% lidocaine was diluted into 1–3% in a human spinal model; therefore, the lidocaine concentration used in this experiment is a potential concentration. Of course, cells are surrounded by fibers or sheaths; however, if lidocaine is injected into a sheath directly, a high concentration of lidocaine will remain in the vicinity of the nerve cells.

However, in attempting to transfer concentrations to the clinical setting, major problems with species differences may occur. The greatest difference between *Lymnaea* and mammals is that the *Lymnaea* has a very large central nervous system (150 μm) that is quite simple in comparison to that of a mammal. Major neurons were identified and named in each. Therefore, each target neuron can be picked up with the use of a micropipette. In addition, in *Lymnaea*, voltage-dependent sodium channels are mostly tetrodotoxin (TTX) resistant, but these *Lymnaea* neurons are blocked by local anesthetics at the same clinical concentration as in mammals [41].

Lymnaea neurons have a lipid bilayer structure that is similar to that in mammals. In addition, the LPeDl neuron has anesthetic-activated potassium currents, such as Ikir, produced by two-pore-domain background K^+ channels, such as TASK and TREK-1, the same as in mammal neurons. Therefore, the membrane potential of LPeD1 is hyperpolarized by general anesthetics in a clinical concentration [42–44].

In this experiment, we isolated and used the identified LPeD1 neuron as a respiratory pattern generator and demonstrated that it has a spontaneous action potential. This pacemaker neuron, similar to other respiratory pacemaker neurons, has a slowly inactivating component of the sodium current and can produce spontaneous action potentials continuously. Therefore, the membrane potential and conditions can be clearly observed for a long time. The major receptors and ion channels that have been identified in *Lymnaea* neurons are similar to those in humans; therefore, isolated and identified *Lymnaea* neurons represent an excellent model for the study of the effects of lidocaine [45, 46].

In conclusion, lidocaine irreversibly depolarizes the membrane potential and induces apoptosis and necrosis in a neuron.

Acknowledgments This work was supported in part by a Grant-in-Aid (No. 21591978) for Basic Scientific Research (C) from the Ministry of Education, Science, and Technology of Japan.

References

1. Lambert LA, Lambert DH. Irreversible conduction block in isolated nerve by high concentrations of local anesthetics. Anesthesiology. 1994;80:1082–93.
2. Rigler ML, Drasner K, Krejcie TC, Yelich SJ, Scholnick FT, DeFontes J, Bohner D. Cauda equina syndrome after continuous spinal anesthesia. Anesth Analg. 1991;72:275–81.
3. Drasner K. Model for local anesthetic toxicity from continuous spinal anesthesia. Reg Anesth. 1993;18:343–8.
4. Gerancher JC. Cauda equine syndrome following a single spinal administration of 5% hyperbaric lidocaine through a 25-gauge Whitacre needle. Anesthesiology. 1997;87:687–9.
5. Sakura S, Kirihara Y, Muguruma T, Kishimoto T, Saito Y. The comparative neurotoxicity of intrathecal lidocaine and bupivacaine in rats. Anesth Analg. 2005;101:541–7.
6. Kasaba T, Onizuka S, Takasaki M. Procaine and mepivacaine have less toxicity in vitro than other clinically used local anesthetics. Anesth Analg. 2003;9:85–90.
7. Onizuka S, Takasaki M, Syed NI. Long-term exposure to local but not inhalation anesthetics affects neurite regeneration and synapse formation between identified *Lymnaea* neurons. Anesthesiology. 2005;102:353–63.
8. Werdehausen R, Braun S, Essmann F, Schulze-Osthoff K, Walczak H, Lipfert P, Stevens MF. Lidocaine induces apoptosis via the mitochondrial pathway independently of death receptor signaling. Anesthesiology. 2007;107:136–43.
9. Johnson ME, Uhl CB, Spittler KH, Wang H, Gores GJ. Mitochondrial injury and caspase activation by the local anesthetic lidocaine. Anesthesiology. 2004;101:1184–94.
10. Onizuka S, Tamura R, Hosokawa N, Kawasaki Y, Tsuneyoshi I. Local anesthetics depolarize mitochondrial membrane potential by intracellular alkalization in rat dorsal root ganglion neurons. Anesth Analg. 2010;111:775–83.
11. Onizuka S, Yonaha T, Tamura R, Kashiwada M, Shirasaka T, Tsuneyoshi I. Lidocaine depolarize mitochondrial membrane potential by intracellular alkalization in rat dorsal root ganglion neurons. J Anesth. 2011;25:229–39.
12. Onizuka S, Kasaba T, Hamakawa M, Ibusuki I, Takasaki M. Lidocaine increases intracellular sodium concentration through voltage-dependent sodium channels in an identified *Lymnaea* neuron. Anesthesiology. 2004;101:110–9.
13. Yagiela JA, Benoit PW, Fort NF. Mechanism of epinephrine enhancement of lidocaine-induced skeletal muscle necrosis. J Dent Res. 1982;61:686–90.
14. Lawrence VS, Marte E, Brown BW, Van Bergen FH. Lidocaine, 2-chlorprocaine and hepatic necrosis. Anesth Analg. 1966;45:55–8.
15. Howl JD, Publicover SJ. Bay K 8644 induced necrosis in murine skeletal muscle in vitro: myofibre breakdown precedes significant alterations of intracellular [Ca] or pH. Acta Neuropathol. 1989;77:634–44.
16. Arrebola F, Zabiti S, Cañizares FJ, Cubero MA, Crespo PV, Fernández-Segura E. Changes in intracellular sodium, chlorine, and potassium concentrations in staurosporine-induced apoptosis. J Cell Physiol. 2005;204:500–7.
17. Belaud-Rotureau MA, Leducq N, Poulletier Macouillard, de Gannes F, Diolez P, Lacoste L, Lacombe F, Bernard P, Belloc F. Early transitory rise in intracellular pH leads to Bax conformation change during ceramide-induced apoptosis. Apoptosis. 2000;5:551–60.
18. Sebbagh M, Renvoizé C, Hamelin J, Riché N, Bertoglio J, Bréard J. Caspase-3-mediated cleavage of ROCK I induces MLC phosphorylation and apoptotic membrane blebbing. Nat Cell Biol. 2001;3:346–52.
19. Chen T, Wang J, Xing D, Chen WR. Spatio-temporal dynamic analysis of bid activation and apoptosis induced by alkaline condition in human lung adenocarcinoma cell. Cell Physiol Biochem. 2007;20:569–78.
20. Yang KT, Pan SF, Chien CL, Hsu SM, Tseng YZ, Wang SM, Wu ML. Mitochondrial Na^+ overload is caused by oxidative stress and leads to activation of the caspase 3-dependent apoptotic machinery. FASEB J 2004;18:1442–4.
21. Van Cruchten S, Van Den Broeck W. Morphological and biochemical aspects of apoptosis, oncosis and necrosis. Anat Histol Embryol. 2002;31:214–23.
22. Doonan F, Cotter TG. Morphological assessment of apoptosis. Methods. 2008;44:200–4.
23. Syed N, Bulloch A, Lukowiak K. In vitro reconstruction of the respiratory central pattern generator of the mollusk *Lymnaea*. Science. 1990;12:282–5.
24. Tchoukalova YD, Harteneck DA, Karwoski RA, Tarara J, Jensen MD. A quick, reliable, and automated method for fat cell sizing. J Lipid Res. 2003;44:1795–801.
25. Brierley MJ, Staras K, Benjamin PR. Behavioral function of glutamatergic interneurons in the feeding system of *Lymnaea*. J Neurophysiol. 1997;78:3386–95.
26. Kits KS, Lodder JC, Veerman MJ. Phe-Met-Arg-Phe-amide activates a novel voltage-dependent K^+ current through a lipoxygenase pathway in molluscan neurons. J Gen Physiol. 1997;110:611–28.
27. Sakakibara M, Okuda F, Nomura K, Watanabe K, Meng H, Horikoshi T, Lukowiak K. Potassium currents in isolated statocyst neurons and RPeD1 in the pond snail, *Lymnaea stagnalis*. J Neurophysiol. 2005;94:3884–92.
28. Hong JR, Lin TL, Hsu YL, Wu JL. Apoptosis precedes necrosis of fish cell line with infectious pancreatic necrosis virus infection. Virology. 1998;250:76–84.

29. Bainton CR, Strichartz CR. Concentration dependence of lidocaine-induced irreversible conduction loss in frog nerve. Anesthesiology. 1994;81:657–67.
30. Kanai Y, Katsuki H, Takasaki M. Graded, irreversible changes in crayfish giant axon as manifestations of lidocaine neurotoxicity in vitro. Anesth Analg. 1998;86:569–73.
31. Kamiya Y, Ohta K, Kaneko Y. Lidocaine-induced apoptosis and necrosis in U937 cells depending on its dosage. Biomed Res. 2005;26:231–9.
32. Friederich P, Schmitz TP. Lidocaine-induced cell death in a human model of neuronal apoptosis. Eur J Anaesthesiol. 2002;19:564–70.
33. Wlodkowic D, Skommer J, Darzynkiewicz Z. Flow cytometry-based apoptosis detection. Methods Mol Biol. 2009;559:19–32.
34. Tsuchiya H, Mizogami M, Ueno T, Takakura K. Interaction of local anaesthetics with lipid membranes under inflammatory acidic conditions. Inflammopharmacol. 2007;15:164–70.
35. Kitagawa N, Oda M, Totoki T. Possible mechanism of irreversible nerve injury caused by local anesthetics: detergent properties of local anesthetics and membrane disruption. Anesthesiology. 2004;100:962–7.
36. Brooks C, Ketsawatsomkron P, Sui Y, Wang J, Wang CY, Yu FS, Dong Z. Acidic pH inhibits ATP depletion-induced tubular cell apoptosis by blocking caspase-9 activation in apoptosome. Am J Physiol Renal Physiol. 2005;289:410–9.
37. Lagadic-Gossmann D, Huc L, Lecureur V. Alterations of intracellular pH homeostasis in apoptosis: origins and roles. Cell Death Differ. 2004;11:953–61.
38. Kim JM, Bae HR, Park BS, Lee JM, Ahn HB, Rho JH, Yoo KW, Park WC, Rho SH, Yoon HS, Yoo YH. Early mitochondrial hyperpolarization and intracellular alkalinization in lactacystin-induced apoptosis of retinal pigment epithelial cells. J Pharmacol Exp Ther. 2003;305:474–81.
39. Ross BK, Coda B, Heath CH. Local anesthetic distribution in a spinal model: a possible mechanism of neurologic injury after continuous spinal anesthesia. Reg Anesth. 1992;17:69–77.
40. Rigler ML, Drasner K. Distribution of catheter-injected local anesthetic in a model of the subarachnoid space. Anesthesiology. 1991;75:684–92.
41. Staras K, Gyóri J, Kemenes G. Voltage-gated ionic currents in an identified modulatory cell type controlling molluscan feeding. Eur J Neurosci. 2002;15:109–19.
42. Franks NP, Lieb WR. Stereospecific effects of inhalational general anesthetic optical isomers on nerve ion channels. Science. 1991;254:427–30.
43. Patel AJ, Honoré E, Lesage F, Fink M, Romey G, Lazdunski M. Inhalational anesthetics activate two-pore-domain background K+ channels. Nat Neurosci. 1999;2:422–6.
44. Lopes CM, Franks NP, Lieb WR. Actions of general anaesthetics and arachidonic pathway inhibitors on K^+ currents activated by volatile anaesthetics and FMRFamide in molluscan neurones. Br J Pharmacol. 1998;125:309–18.
45. Winlow W, Spencer GE, Syed NI, Qazzaz MM. Modulation of reconstructed peptidergic synapses and electrical synapses by general anaesthetics. Toxicol Lett. 1998;100:77–84.
46. Hamakawa T, Feng ZP, Grigoriv N, Inoue T, Takasaki M, Roth S, Lukowiak K, Hasan SU, Syed NI. Sevoflurane induced suppression of inhibitory synaptic transmission between soma–soma paired *Lymnaea* neurons. J Neurophysiol. 1999;82:2812–9.